Wavefront Control of High-Power Laser Beams for the National Ignition Facility (NIF)

R. Zacharias, E. Bliss, S. Winters, R. Sacks, M. Feldman, A. Grey, J. Koch, L. Lund, D. Smith, C. Stolz, J. Toeppen, L. Van Atta, and B. Woods

U.S. Department of Energy

Lawrence
Livermore
National
Laboratory

September 22, 1999

DISCLAIMER

Wavefront Control of High-Power Laser Beams for the National Ignition Facility (NIF)

Richard Zacharias[a*], Erlan Bliss[a], Scott Winters[a], Rick Sacks[a], Mark Feldman[a], Andrew Grey[a], Jeff Koch[a], Lance Lund[b], Doug Smith[b], Chris Stolz[a], John Toeppen[a], Lewis Van Atta[a], and Bruce Woods[a]

[a]Lawrence Livermore National Laboratory, 7000 East Ave, Livermore, CA 94550
[b]University of Rochester Laboratory for Laser Energetics, 250 East River Road, Rochester, NY 14623

ABSTRACT

The use of lasers as the driver for inertial confinement fusion and weapons physics experiments is based on their ability to produce high-energy short pulses in a beam with low divergence. Indeed, the focusability of high quality laser beams far exceeds alternate technologies and is a major factor in the rationale for building high power lasers for such applications.

The National Ignition Facility (NIF) is a large, 192-beam, high-power laser facility under construction at the Lawrence Livermore National Laboratory for fusion and weapons physics experiments. Its uncorrected minimum focal spot size is limited by laser system aberrations. The NIF includes a Wavefront Control System to correct these aberrations to yield a focal spot small enough for its applications. Sources of aberrations to be corrected include prompt pump-induced distortions in the laser amplifiers, previous-shot thermal distortions, beam off-axis effects, and gravity, mounting, and coating-induced optic distortions. Aberrations from gas density variations and optic-manufacturing figure errors are also partially corrected.

This paper provides an overview of the NIF Wavefront Control System and describes the target spot size performance improvement it affords. It describes provisions made to accommodate the NIF's high fluence (laser beam and flashlamp), large wavefront correction range, wavefront temporal bandwidth, temperature and humidity variations, cleanliness requirements, and exception handling requirements (e.g. wavefront out-of-limits conditions).

KEYWORDS: Wavefront Control, Wavefront Correction, Adaptive Optics, High Power Lasers

1. INTRODUCTION

A primary requirement for the NIF is that each beam shall deliver its design energy into a 600 μm inertial confinement fusion (ICF) target. The total design energy for 192 beams is 1.8 Megajoules. A system performance goal is that 500 Terawatts of total power should be placed within a 250 μm focal spot at the target plane.

In order to meet the spot-size requirement and goal, the NIF subsystems are designed to limit wavefront aberrations. Optics are made to stringent specifications for rms surface gradient, power spectral density, and roughness[1]. Stringent specifications are also maintained for optical component mounting. The NIF subsystems are also designed to mitigate the effects of temperature and humidity variations and vibrations[2]. An active alignment system accurately points the beams into the target[3]. Even with these efforts , the NIF spot-size requirement and goal could not be met without a Wavefront Control System.

2. THE NIF WAVEFRONT CONTROL SYSTEM

A block diagram of the NIF main laser optical system is shown in Figure 1, with the NIF Wavefront Control System components highlighted in black. The NIF preamplifier 1ω (1.053 μm) beam enters the main laser chain near the focus of the transport spatial filter (TSF), directed away from the target. The beam is collimated as it exits the filter and passes through

---

the boost amplifier heading towards the laser main amplifier cavity. A Pockels cell allows the beam to enter the cavity, where it makes four passes through the main amplifier before the Pockels cell is switched, allowing the beam to exit. The beam then passes through the boost amplifier and the TSF and heads towards the target chamber. There beam is frequency-converted to 3ω (351 nm) and focused onto the target.
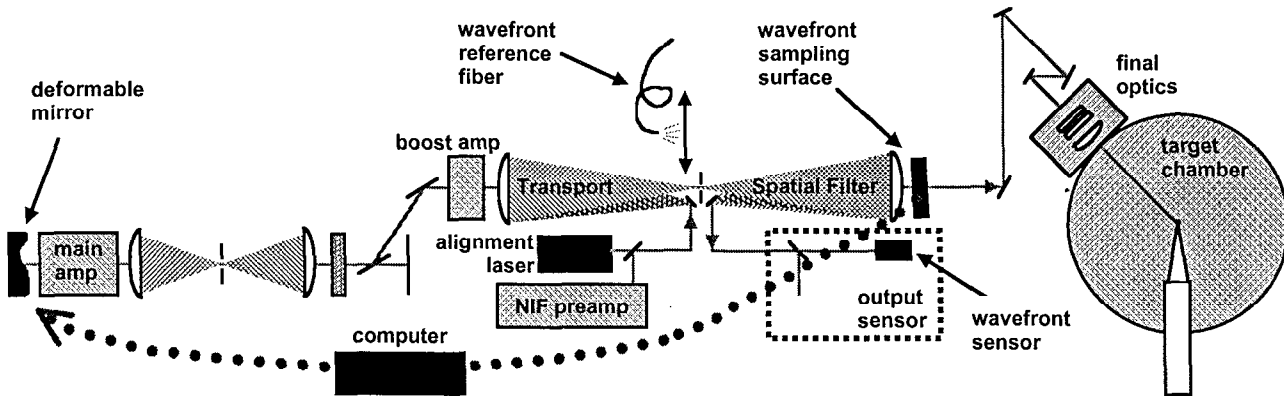

Figure 1. Overview of components in the NIF.

Wavefront control functions are implemented as follows. A 1ω cw probe beam is co-aligned with the NIF beam prior to injection into the main laser. The probe beam follows the NIF beam path. A 39-actuator large-aperture deformable mirror (DM) operates at the far end of the laser cavity where the beam bounces twice. This two-bounce configuration doubles the effective stroke of the DM. At the TSF output, a tilted sampling surface reflects a small fraction of the beam towards a pick-off mirror near TSF focus that sends the sampled beam through relays to the Output Sensor. Within the Output Sensor, a 77-lenslet Hartmann sensor (HS) measures the wavefront. The Hartmann sensor's video output is read by a frame-grabber in the wavefront control computer. The computer calculates the surface displacements to be applied to the deformable mirror to correct the wavefront aberrations in the beam.

There are several functions that the wavefront system must perform. These include: 1) Control the 1ω output wavefront (including pointing) of each beam in the time immediately preceding a laser system shot, 2) Apply compensation for previously-measured pump-induced wavefront distortion, 3) Measure beam output wavefront during a laser system shot, and 4) Control the output wavefront (excluding pointing) during routine system operations between shots.

Wavefront control sub-system design requirements (SSDRs) flow down from the NIF primary requirements, which include the spot size requirement[4,5]. Other factors that influenced the Wavefront Control System SSDRs included system cost and experience with the wavefront control of Beamlet, the single-beam NIF prototype laser[6]. These SSDRs are shown in Table 1. The number of actuators is a major cost driver for the system because the cost and complexity of the wavefront sensor and the computer control system also must increase by approximately the same factor. The 39-actuator mirror is the largest that the budget would support. Based on prototype tests and performance models, the Wavefront Control System is expected to meet all SSDRs, except initially the closed-loop bandwidth. The bandwidth is processor-limited, and it is expected that by the time NIF is integrated, faster processors will be available to meet the requirement without major changes to the software or hardware architecture.

In order to meet its spot-size requirement, all NIF system aberrators must be minimized (within affordable limits), and it must be assured that the Wavefront Control System has the stroke required to correct the worst-case aberrations. To this end, a wavefront budget was established, wherein each aberration contributor was expressed in terms of its first 15 Zernike polynomials (minus the three that describe tilt and piston) and the sum taken. The stroke budget resulting from this analysis is shown in Figure 2, and was used as a tool to assign aberration limits to the various NIF subsystems. Note that about 31% (4.6 waves) of stroke are reserved as margin and that this budget does not include switchyard and final optics aberrations, or the deformable mirror residual error, which the wavefront system cannot control. Also this budget does not address system performance for high spatial frequency aberrations, which is addressed in Section 9 below using propagation models.

Requirement	Value	Expected Performance
Max residual low spatial frequency angle	±20 μradians at 1ω	±20 μradians at 1ω
Maximum open-loop time before a shot	1 second	1 second
Minimum closed loop bandwidth	1 Hz	0.5 Hz (upgrade to 1 Hz)
Number of actuators	39	39
Compensation range for simple curvature (double-pass reflected wavefront)	15 waves at 1ω	15 waves at 1ω
Order of aberrations corrected	≤ 4th order	≤ 4th order
Measurement accuracy at 1ω	0.1 waves	0.1 waves
Lenslet spacing	≤ 1/2 demagnified actuator spacing	≤ 1/2 demagnified actuator spacing

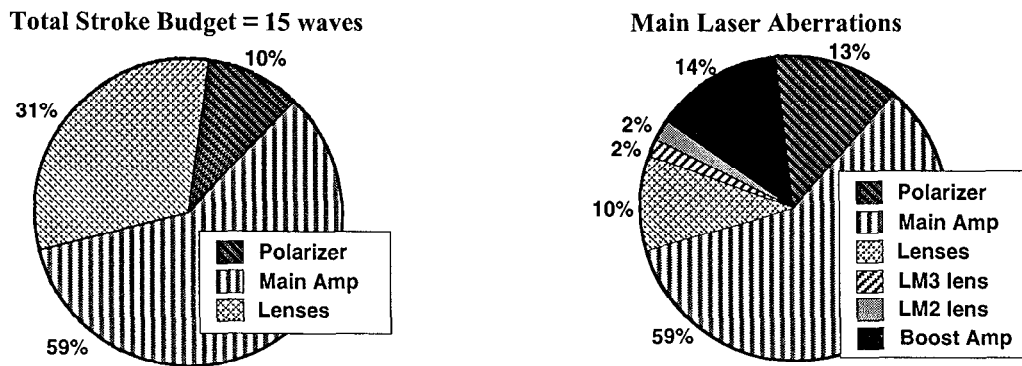Table 1. NIF Wavefront Control System Subsystem Requirements.

Figure 2. Adaptive optic stroke budget, a) Total budget, b) Main laser aberrations.

The Wavefront Control System consists of five subsystems for each beam. These are the deformable mirror, the Shack-Hartmann wavefront sensor, the wavefront control computer system, the wavefront reference, and the "t_0-1" system. The "t_0-1" system consists of a set of fast actuators to quickly reconfigure the NIF from the wavefront control mode to shot mode. The computer control system, wavefront sensor, wavefront reference, and "t_0-1" system have been described in previous publications, and are summarized in this paper[7,8,9,10].

The NIF Wavefront Control System is a new design, but many of the design concepts evolved from LLNL experience with previous laser systems built at LLNL[6,8]. Portions of the Wavefront Control System are integrated with NIF alignment and diagnostic functions to reduce cost[11]. For example, the system uses the same laser for the wavefront control probe beam as is used for laser alignment. The wavefront sensor is contained in the NIF diagnostic output sensor so as to avoid the cost of separate beam sampling and relaying optics. The wavefront reference fiber also doubles as an alignment reference.

3. DEFORMABLE MIRROR

The deformable mirror (DM) must meet stringent performance requirements and must operate in a severe environment. Some of the features and requirements of the DM are shown in Table 2 and some parameters of the environment within which it must operate are shown in Table 3. A particularly stringent goal is that the DM should have less than 0.025 waves of rms residual error between the DM surface and a true flat surface when the mirror is commanded to be flat in closed loop. The 10 J/cm^2 flashlamp fluence is a particularly severe environmental parameter.

Features and Requirements	
39 control points in a hexagonal pattern	Clear aperture of 400 mm by 400 mm
0.025 waves rms surface residual error (closed loop to flat)	Replaceable actuators
Size and weight compatible with NIF packing density	Correction stroke ≥ 4 waves (surface)
Coating reflectivity ≥ 99.5%	Coating: 0.2% ≤ Transmission ≤ 0.5%
Open loop actuator bandwidth ≥ 100 Hz	Actuator linearity ≤ 8%
Actuator lifetime ≥ 10^9 cycles	

Table 2. Deformable mirror features and requirements.

Environment
10 J/cm^2 laser pump flashlamp fluence
EMI of 8 gauss and 13 V/m in a 200 μsec pulse just prior to the laser shot
Relative humidity ≤ 3%
Class 50 cleanliness on the optical surface and class 100 for the assembly

Table 3. Deformable mirror environment requirements.

A photograph and concept sketch of the NIF deformable mirror is shown in Figure 3. This DM is the latest of numerous generations of DMs that have been built at LLNL. It employs PMN actuators that move a glass faceplate by pushing against a stiff metal reaction block. The prototype DM faceplate was fabricated by Zygo and coated by Spectra Physics, and the actuators were supplied by Xinetics.
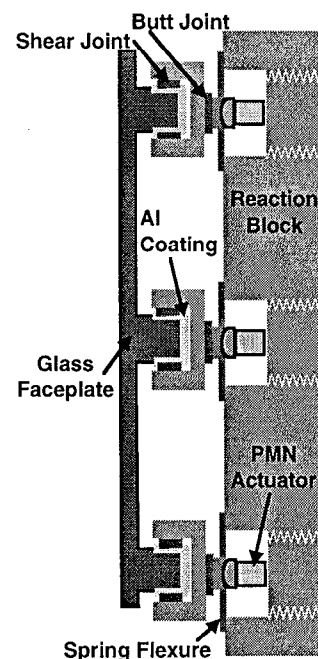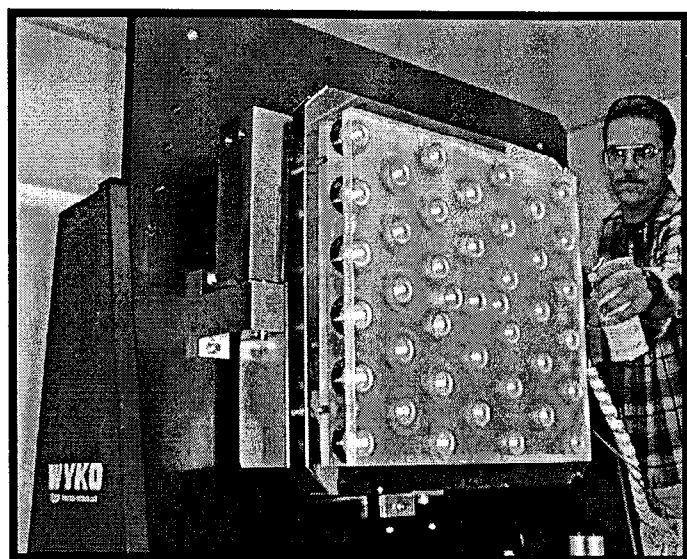

Figure 3. Photograph and concept sketch of the NIF DM showing major components.

There are several major features designed into this DM to allow it to meet its fluence, precision, and reliability requirements. First, the NIF DM actuators are held in constant compression by a disk flexure rather than being directly connected to the faceplate. Actuators directly connected to the faceplate work against neighboring actuators putting some of them in tension. Tension in the actuators can cause microcracks to propagate leading to latent failures. The disk flexures also protect the actuators from the shear load of the faceplate. Second, the faceplate is held to the actuator indirectly by an epoxy shear joint between the aluminum-coated DM posts and a stainless steel cup. Previous flashlamp exposure tests had demonstrated that a simple, unprotected butt joint would be destroyed by NIF's extreme flashlamp fluence. With this approach, the joint is on the side of the post, and the geometry and total internal reflection limit the fluence seen by the aluminum coating. The aluminum

protects the Hysol 9330 epoxy. This actuator connection approach was successfully tested on the previous-generation large-aperture mirror in Beamlet, a one-arm laser prototype of the NIF. Third, the faceplate high-reflectance coating is applied prior to DM assembly rather than afterwards. In order to survive the high-fluence NIF beams, the DM employs a Hafnia-Silica high-reflectance multilayer dielectric coating. This coating is applied at high temperatures that would destroy the epoxy bonds in the actuator force train if the coating was applied after DM assembly. Unfortunately, the stress applied by the coating can be significant and is a function of humidity and aging. Coating stress can increase DM residual error and is a significant challenge for this design. Approaches to minimize coating-stress-induced distortions are being investigated at the Laboratory for Laser Energetics at the University of Rochester. Fourth, a butt joint is used to attach the mirror cups to the reaction block. Compared to a direct connection or flexure connection, this approach makes the DM much less susceptible to front-face distortions from misalignment-induced moments on the mirror posts.

The PMN actuators must have enough stroke to move the faceplate over the required 4 µm of surface displacement while allowing for the inefficiency in the force train. The actuators do not have a large stroke margin. A concern is that with time and flashlamp exposure, the epoxy bonds in the cups will relax and the DM surface will creep to the point that the actuator stroke margin is used up. To assess that possibility, a series of experiments were conducted using an interferometer to measure the relaxation of the joint after flashlamp exposure. In these experiments, test articles were made up of aluminum-coated glass posts epoxied to stainless steel cups, simulating the post-to-cup joint of the mirror. The joint was placed into tension using a Bellville washer. The tension was calibrated and set to the maximum expected of a joint in the DM. An interferometer was then uses to measure the peak-to-valley displacement of the front face of the test article as it is warped to a concave surface due to the tension of the washer. The test articles were then exposed to 1000 flashlamp shots simulating the NIF fluence at the DM location. Interferometer measurements made after exposure showed that creep was much less than a micron. One thousand shots represent about 5% of the total number of shots expected over the NIF lifetime. Further tests with more shots at a higher fluence to establish margin are planned.

Numerous other tests were conducted to assure that the DM would survive the NIF environment. Actuators were tested to assure that they would survive the EMI of the laser flashlamps during the shot. Candidate DM epoxies were tested for mass loss. Since the DMs resides within the same cavity as the NIF main amplifier laser slabs, volatile and particulate emissions generated by the DMs must be kept low so as to not corrupt the slab and coated optic surfaces, which would cause damage during a high power shot. The Hysol 9330 epoxy was shown to have excellent low-mass loss performance. Since it will be difficult to clean all of the nooks and crannies of the actuator force trains and of the actuator wiring after assembly, the DM design includes "cleanliness shields" that cover its back and sides. These easy-to-clean outer shell components will encapsulate the hard-to-clean interior.

4. WAVEFRONT SENSOR

The NIF will employ miniature Shack-Hartmann sensors to detect wavefront[10]. A sketch depicting the operation of the sensor is shown in Figure 4. Each lenslet generates a focus spot whose position displacement is directly proportional to the local deviation from collimation of the portion of the beam that impinges on it. The sensor has been demonstrated to resolve 0.1 wave at 1.053 µm. The prototype sensor uses an array of lenslets manufactured by MEMs Optical Systems Inc. Index matching fluid is used to adjust the lenslet focal length to the value that provides the required sensitivity and range.

In the NIF, each Output Sensor is shared by two beams. For most diagnostics, the operator selects which beam is to be viewed, but since the Wavefront Control System must operate simultaneously for all beams, two beams are spatially multiplexed onto one sensor[11]. The sensor monitors a beam that has been demagnified by the pick-off and is relay imaged to be somewhat smaller than one-half of the CCD camera array, as shown in Figure 4b.

5. WAVEFRONT REFERENCE

The Wavefront Control System is calibrated by inserting a wavefront reference fiber at the focal point of the TSF. This concept is shown in Figure 5. Since the fiber light source is smaller than the TSF diffraction-limited focal spot, the spot pattern at the Hartmann sensor when viewing the fiber reference beam is the same as the pattern the sensor would see when viewing the probe beam if all upstream system components had diffraction-limited performance. The aberrations that are seen with the reference inserted (imperfections in the separations of the lenslet array focal points) are due to aberrations in the measuring system (sampling surface, relay optics, output sensor optics, and the sensor itself). By designing the control system to use the sensor focal spot image of the wavefront reference as the target to which the system wavefront is controlled, the system tries to generate, as closely as it can with a limited number of actuators, a perfect focal spot in the TSF.

This implies that aberrations in all the optics beyond the TSF focus, including the TSF output lens, are uncorrected by the Wavefront Control System.
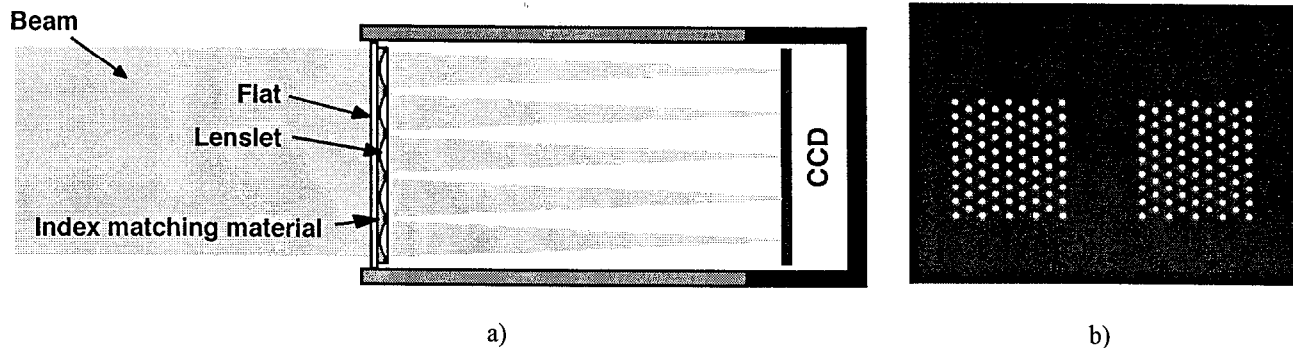

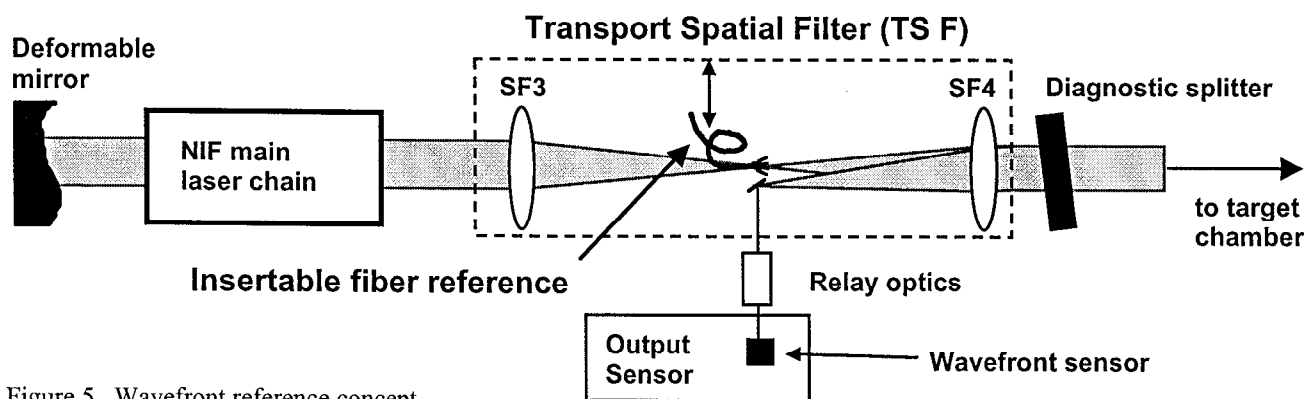Figure 4. a) Shack-Hartmann sensor concept sketch. b) Focal plane image of dual-beam Hartmann sensor.

Figure 5. Wavefront reference concept.

6. WAVEFRONT COMPUTER CONTROL SYSTEM

A functional block diagram of the NIF wavefront control computer is shown in Figure 6. Initially, the wavefront reference is inserted and its spot positions are measured by the Hartmann sensor, creating a reference spot position file. Next, the wavefront reference source is replaced by the probe beam and the Wavefront Control System is calibrated by an on-line procedure. Each of the 39 actuators is individually poked and pulled relative to the best-flat starting point. The offset for each Hartmann spot is thus related to the displacement of each actuator. From this information, a gain matrix relating actuator movement to Hartmann sensor focal spot movement is derived[7].

Once the calibrations are complete, the loop is closed wherein the measured Hartmann offsets from the reference positions are multiplied by the gain matrix yielding the actuator offsets to control the mirror to flat (with appropriate loop gain for stability). This is the configuration used during alignment. After alignment is complete and the shot sequence has begun, an additional Hartmann offset file is subtracted from the wavefront sensor data prior to being applied to the gain matrix. These additional offsets represent the uncorrected prompt pump-induced wavefront aberrations measured on a previous shot. By subtracting out these offsets, the wavefront is set to the conjugate of the expected prompt aberration of the upcoming shot. Thus, at shot time, the wavefront is flat.

The NIF wavefront control computer system uses modular hardware and object oriented software. The NIF facility is expected to be operated for 30 years, and software and hardware changes are expected over that time. By using a modular hardware and software architecture, system maintainability is improved significantly.

To achieve the 0.5 Hz bandwidth, the wavefront sensor is read at a 10 Hz rate. A planned upgrade to 30 Hz should allow the goal of 1Hz bandwidth to be achieved. The sensor is read-out in standard RS-170 video, which is read by an Active Imaging Snapper 24 frame grabber. The digitized image is fed into a SPARCengine AXI computer that calculates centroids for all 77

lenslet spots and then calculates their offsets from the reference positions. This information is sent via a dedicated ethernet line to the Motorola MVME 2306 controller that calculates the required DM actuator displacements. Each image processor services four Hartmann sensors and eight beams. Each control computer services four DMs.
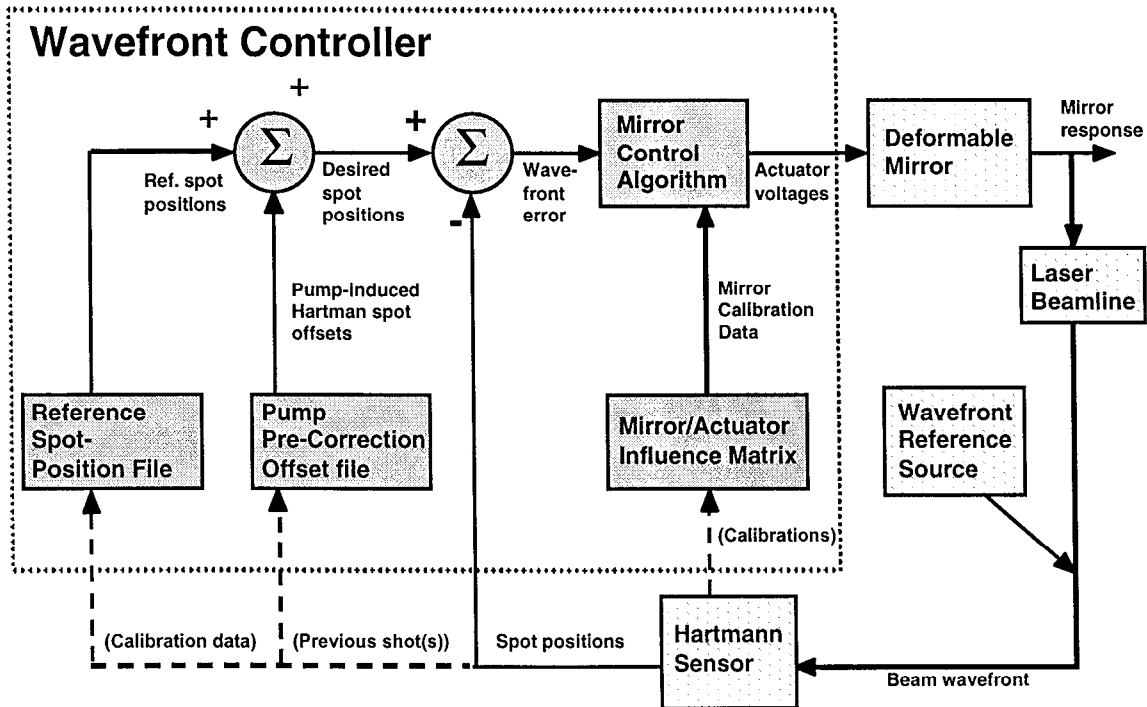

Figure 6. The NIF Wavefront Control System functional block diagram.

As will be shown below in Section 9, if the Wavefront Control System is not operating properly, the beam can damage the NIF by applying too much energy to filter pinholes, and, by diffraction, too much localized energy to system optics. Therefore, the Wavefront Control System includes an exception handling algorithm that continually monitor the probe-beam wavefront during shot preparations until one second prior to the shot, and precludes the shot if the measured wavefront is out of limits.

7. WAVEFRONT SYSTEM TEST FACILITY

The Wavefront Control System is tested at LLNL in a special Fizeau interferometer system that can view the deformable mirror surface while the wavefront control loop is closed. A standard practice in interferometer design is to minimize the length of the interferometer cavity by keeping the partially-transmitting reference surface adjacent to or as close as possible to the measured surface. This minimizes coherence degradation, air path density variations, and differential vibrations. Unfortunately, this conflicts with the requirement for this application that the Hartmann sensor see only one surface - the DM to be controlled. This requirement drove the design to the configuration used.

A block diagram of the interferometer system is shown in Figure 7. The YAG beam from a commercial 4" interferometer head (Phase Shift Technologies) returns a portion of its beam at the transmission flat before the beam passes through a splitter and is expanded by a high-quality Kepler telescope. The expanded beam reflects off of the deformable mirror (or a reference flat) and returns through the telescope. On the return path, the splitter sends a portion of the beam to the Hartmann sensor. Since the Hartmann sensor beam sample is taken within the interferometer cavity, it sees only one reflective surface, and thus the loop can be closed. The reference flat replaces the DM for a reference measurement used to subtract out the aberrations in the interferometer path added by the splitter, fold mirrors, and telescope. The entire system resides on a granite slab within a temperature and humidity controlled enclosure to minimize vibration and air density variation effects which otherwise would be problematic due to the large interferometer cavity.

The measurement system was used to measure DM influence functions and residual error. An influence function is the surface of the entire DM when a single actuator is displaced a unit distance. A typical measured influence function and residual error of the DM are shown in Figure 8. Note that the residual error of .034 waves is above the goal of .025 waves.
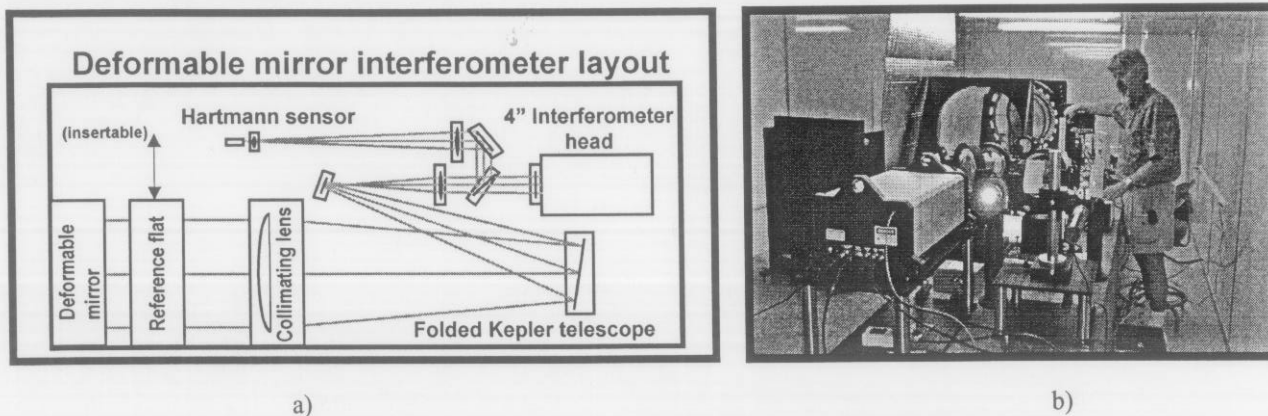

a)

b)

Figure 7. Wavefront Control System Test Facility. a) Layout, b) Photograph.

8. PROPAGATION MODELING OF LASER SPOT SIZE

A model of the entire NIF beam-line was constructed, using the Prop92 laser propagation code developed at LLNL, and used to evaluated Wavefront Control System performance. A model of the DM was constructed using the measured influence functions for all 39 actuators and the measured residual error. Essentially, the DM surface is modeled as the superposition of the 39 actuator influence functions plus the measured residual error. The model was validated with large DM experiments on Beamlet and is described in detail in a paper by Sacks, et al[12].

a)

b)
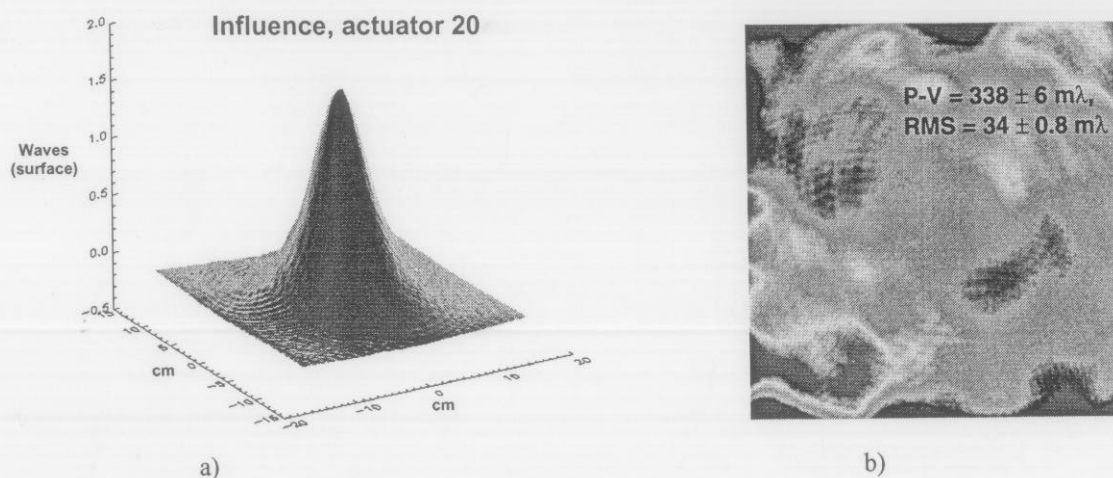
Figurs 8. a) Typical measured influence function, b) Typical measured residual error.

With only 39 actuators, the DM is designed primarily to correct low spatial frequency aberrations. Major low spatial frequency system aberrators include Seidel terms from lens figuring and misalignment, prompt and thermal distortions of amplifier slabs, cavity and polarizer distortions from coating stress, and polarizer and mirror distortions from mounting and gravity sag. To demonstrate Wavefront Control System performance, the NIF was modeled first with only these four aberrations.

The predicted NIF tripled output results are shown Figure 9 with the Wavefront Control System turned off. The beam divergence spreads 80% of the total laser power over a 37 µradian spot, much larger than the ~20 µradians required. Furthermore, the beam nearfield has high contrast (due to clipping from poor angular control) and the peak fluence at the final optics has exceeded the maximum "red-line" damage value. The Wavefront Control System in the model was then

turned on, and the results are shown in Figure 10. Now the system focuses 80% of its energy into a much smaller 10.5 μradian spot. The nearfield has much lower contrast, and the peak does not exceed red-line. Thus, the Wavefront Control System allows much more laser energy to gainfully (pun intended) enter the target. Figure 10 shows the predicted NIF uncorrected output wavefront, the model deformable mirror surface, and the predicted residual error after correction.
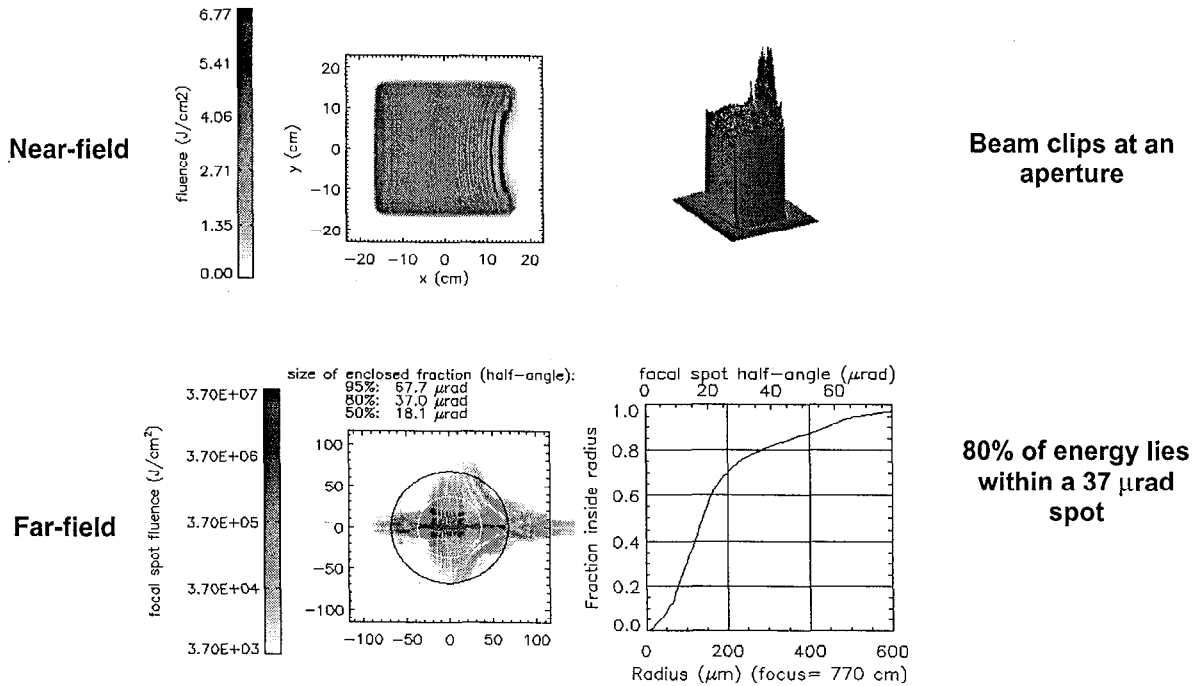

Near-field

Beam clips at an aperture

Far-field

size of enclosed fraction (half—angle):
95%: 67.7 μrad
80%: 37.0 μrad
50%: 18.1 μrad

80% of energy lies within a 37 μrad spot

Figure 9: Predicted output near-field and far-field with the Wavefront Control System turned off.

Uncorrected output wavefront

weighted rms(waves)= 0.763
pk—vl(waves)= 5.763
strehl ratio= 0.0442

Deformable mirror surface shape

rms(waves)= 0.260
pk—vl modulation(waves)= 1.469
max curvature= 0.0464 waves/cm^2

Residual wavefront

weighted rms(waves)= 0.0759
pk—vl(waves)= 0.554
strehl ratio= 0.767

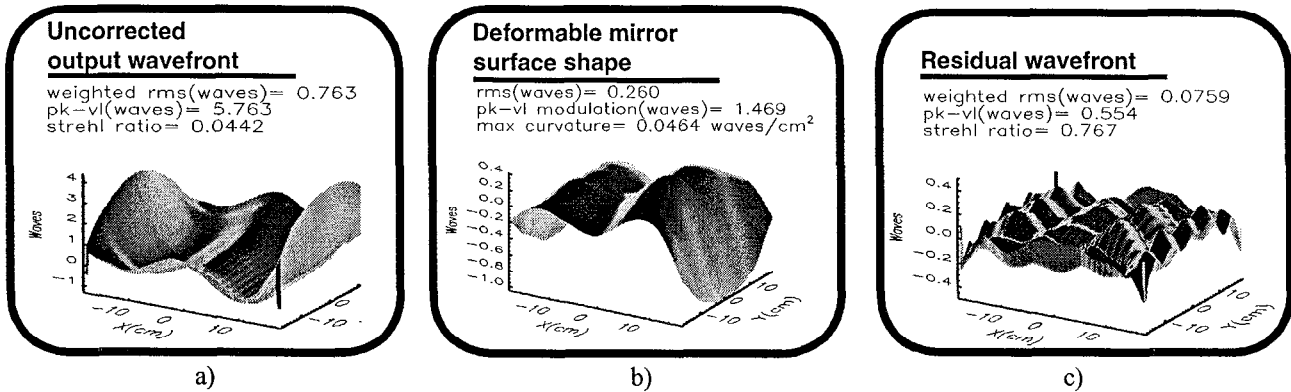a)   b)   c)

Figure 10. : Model predictions of: a) Output wavefront with 4 aberrators, b) DM correction surface, c) Residual error.

The NIF system model was then upgraded to include all significant sources of aberration. Modeled elements included all optics, beam tilts and offsets, mounting aberrations (from FEA models), and the real-time correction algorithm including Hartmann sensor limitations, detector thresholding, and baseline actuator positions. Elements based on Beamlet measurements included prompt and slow amplifier thermal distortions, frequency conversion with nonlinear wavefront effects, and gas inhomogeneity with "t_0-1" effects. Elements base on measurements of sample components included large optic figure errors, polarizer and mirror coating stress aberrations, and transport and final-optics assembly aberrations. The far-field performance of the system based on the complete model is shown in Figure 11. This analysis shows that with the baseline components, the system will deliver 410 Terawatts into a 250 μm target, compared to a goal of 500 TW.

Near-field

Beam is not clipped

Far-field

size of enclosed fraction (half-angle):
95%: 29.9 μrad
80%: 10.5 μrad
50%: 5.7 μrad

80% of energy lies within a 10.5 μrad spot
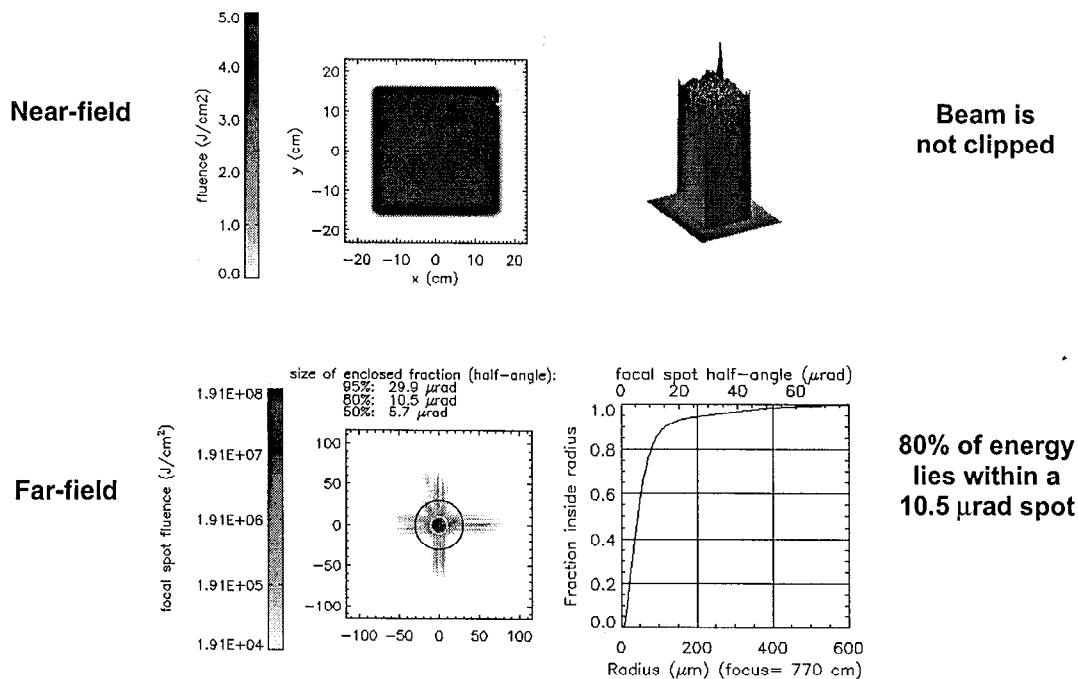
Radius (μm) (focus= 770 cm)

Figure 10. : Predicted output near-field and far-field with the Wavefront Control System turned on.

Parametric studies were conducted to investigate the sources of aberration that promote the largest increases in target spot size. First, the effect of the DM was investigated, since the prototype residual error was high. Figure 12 shows the power into a 250 μm target as a function of DM residual error when it was scaled up and down from the measured value. This shows that the higher-than-goal residual error only decreased the power into the target by about 1% and that the NIF would not meet its spot size goal with the current baseline system aberrations, even with a perfect, zero-residual-error DM.

Next, a parameter study was conducted by cumulatively reducing each of the various system aberrations that contained significant high spatial frequencies. This included reducing the rms gradient specification for spatial frequencies with periods above 33mm by a factor of 5/7, reducing the of-order-10-mm size optic figure errors by 13/17, cutting front-end aberrations by half, and cutting turbulence by half. The result is shown in Figure 13, along with a curve where turbulence is turned off completely. This shows that turbulence and optic figure errors are major contributors to the NIF spot size.

size of enclosed fraction (half-angle):
95%: 46.6 μrad
80%: 28.2 μrad
50%: 16.4 μrad
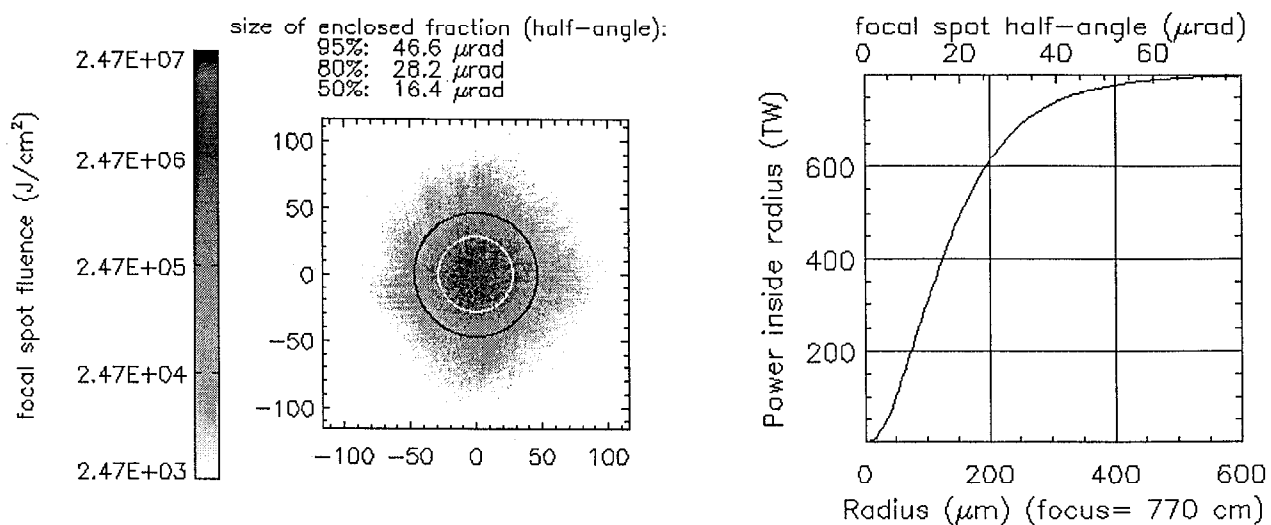
Radius (μm) (focus= 770 cm)

Figure 11. Predicted 3ω output far-field of the NIF using a complete system model and current baseline aberrations.
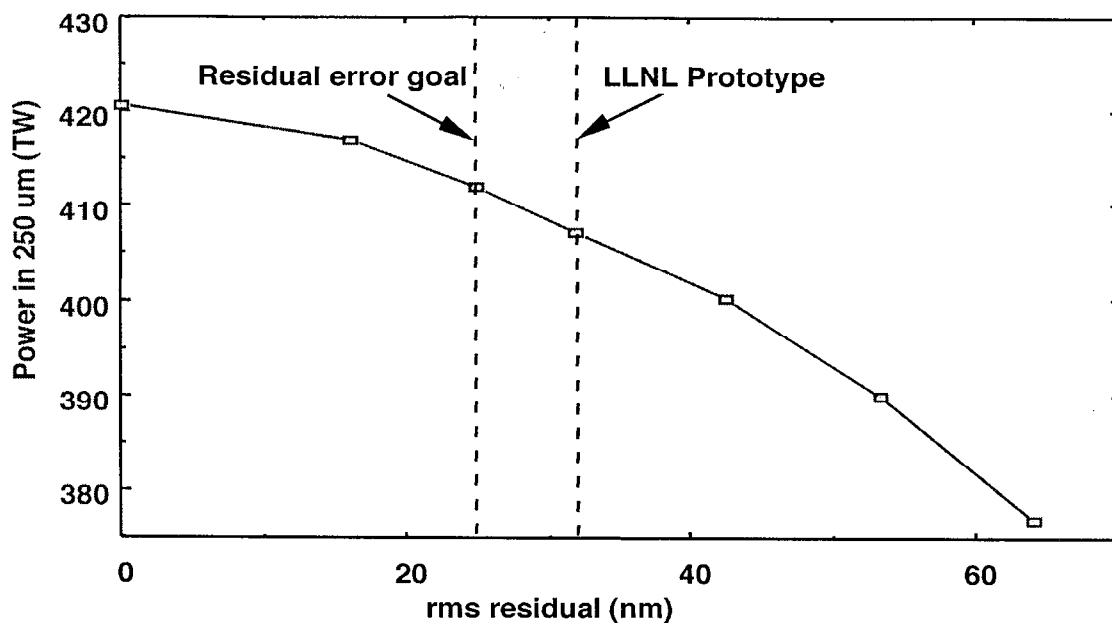
Figure 12. Predicted 3w output power into a 250 μm target as a function of DM residual error.
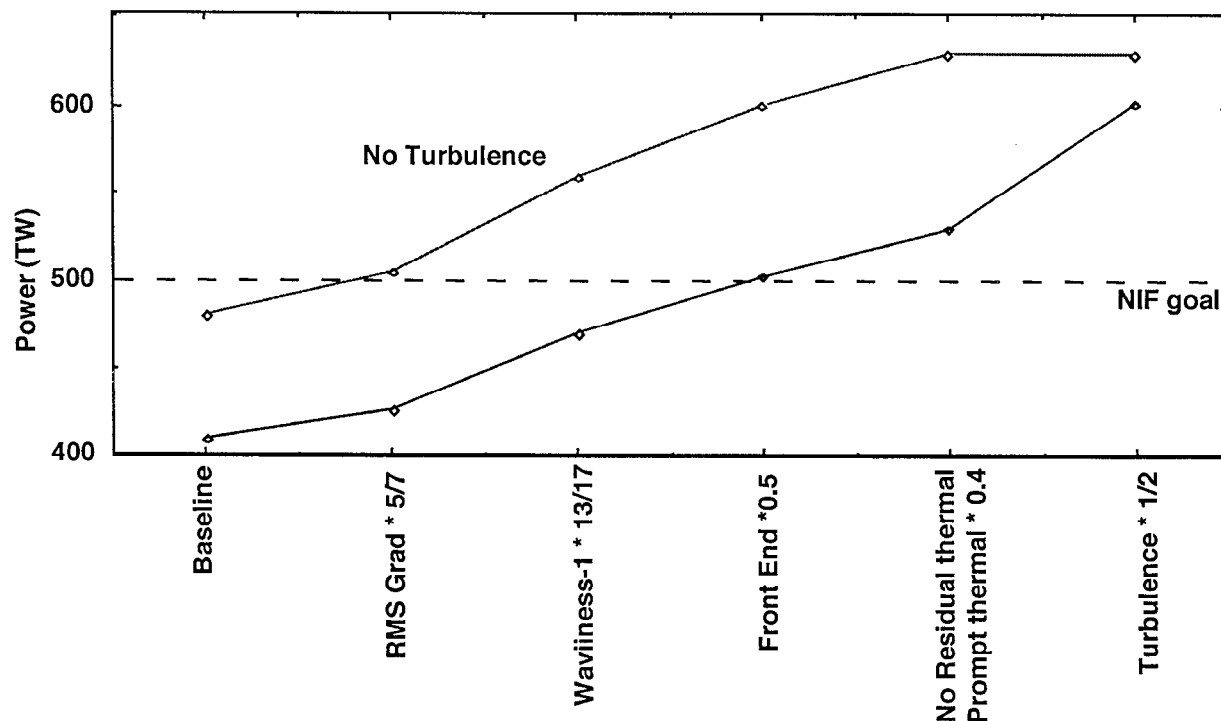

Figure 13. Sensitivity of predicted power to the NIF target as various aberration sources are cumulatively reduced.

SUMMARY

The NIF Wavefront Control System was described emphasizing special features designed in to meet the needs of a high power laser facility. Prototype tests and computer propagation models were used to evaluate system performance. Prototype measurements showed that the Wavefront Control System met all expected performance requirements, except that the DM residual error was slightly over the goal. Propagation model analyses demonstrated that the NIF will meet its spot size

requirement and will approach its spot size goal. Analyses also showed that the prototype DM residual error is not a strong contributor to beam divergence, compared to gas turbulence and small spatial frequency optic figure errors. The NIF project is addressing all of these areas to improve spot size performance.

REFERENCES

1. J.K. Lawson, et al., *NIF Optical Specifications – The Importance of the RMS Gradient Specification*, Proceedings of SPIE, Solid State Lasers for Application to Inertial Confinement Fusion, Third Annual International Conference- June 7-12, 1998 Monterey Conference Center, Monterey, California, Volume 3492.

2. D.J. Trummer, R.J. Foley, F.S. Shaw, *Stability of Optical Elements in the NIF Target Area Building*, Proceedings of SPIE, Solid State Lasers for Application to Inertial Confinement Fusion Third Annual International Conference- June 7-12, 1998 Monterey Conference Center, Monterey, California, Volume 3492.

3. S.C. Sommer and E.S. Bliss, *Beam Position Error Budget Developed for NIF*, Proceedings of SPIE, Solid State Lasers for Application to Inertial Confinement Fusion Third Annual International Conference- June 7-12, 1998 Monterey Conference Center, Monterey, California, Volume 3492.

4. W.H. Williams, et al., *NIF's Basic Focal Spot for ICF Shaped Temporal Pulse*, Proceedings of SPIE *s*, Solid State Lasers for Application to Inertial Confinement Fusion Third Annual International Conference- June 7-12, 1998 Monterey Conference Center, Monterey, California, Volume 3492.

5. W.H. Williams, et al., *NIF's Basic Focal Spot for Flat In Time Pulse*, Proceedings of SPIE *s*, Solid State Lasers for Application to Inertial Confinement Fusion Third Annual International Conference- June 7-12, 1998 Monterey Conference Center, Monterey, California, Volume 3492.

6. B.M. Van Wonterghem, et al., *Beamlet Pulse Generation and Wavefront Control System*, Inertial Confinement Fusion Quarterly Report, Volume 5, Number 1, Oct.-Dec. 1994.

7. J.T Salmon, et al., *Active and Adaptive Optical Systems* (SPIE – International Society for Optical Engineering, Bellingham, WA, 1991:Proc. SPIE 1452) pp.459-467.

8. R.A. Zacharias, *The National Ignition Facility (NIF) Wavefront Control System*, Proceedings of SPIE, Solid State Lasers for Application to Inertial Confinement Fusion Third Annual International Conference- June 7-12, 1998 Monterey Conference Center, Monterey, California, Volume 3492.

9. R. Hartley, et al., *Wavefront Correction for Static and dynamic aberrations to within 1 second of the system shot in the NIF Beamlet demonstration facility*, Proceedings of SPIE, Solid State Lasers for Application to Inertial Confinement Fusion Second Annual International Conference- October 22-25, 1996 Paris, France.

10. J.S. Toeppen, E.S. Bliss, T.W. Long, S.T. Salmon, *A Video Hartmann Wavefront Diagnostic that Incorporates a Monolithic Microlens Array*, Proceedings of SPIE, SPIE International Symposium on Optical Applied Science and Engineering, July 21-26, 1991, San Diego, California.

11. E.S. Bliss, et al., *Design Process for NIF Laser Alignment and Beam Diagnostics*, Proceedings of SPIE, Solid State Lasers for Application to Inertial Confinement Fusion Third Annual International Conference- June 7-12, 1998 Monterey Conference Center, Monterey, California, Volume 3492.

12. R. Sacks, et al., *Application of Adaptive Optics for Controlling the NIF Laser Performance and Spot Size*, Proceedings of SPIE, Solid State Lasers for Application to Inertial Confinement Fusion Third Annual International Conference- June 7-12, 1998 Monterey Conference Center, Monterey, California, Volume 3492.